

Supporting Information

Self-Assembly of Star-Shaped Heteropoly-15-Palladate(II)

Natalya V. Izarova,^a Rosa Ngo Biboum,^b Bineta Keita,^b Maria Mifsud,^c
Isabel W.C.E. Arends,^c Geoffrey B. Jameson,^d and Ulrich Kortz^{*,a}

^a Jacobs University, School of Engineering and Science, P. O. Box 750 561, 28725 Bremen, Germany. Fax: +49 421 200 3229; Tel: +49 421 200 3235; E-mail: u.kortz@jacobs-university.de

^b Laboratoire de Chimie Physique, UMR 8000, CNRS, Equipe d'Electrochimie et Photoélectrochimie, Université Paris-Sud, Bâtiment 350, 91405 Orsay Cedex, France.

^c Laboratory for Biocatalysis and Organic Chemistry, Delft University of Technology, Julianalaan 136, 2628 BL Delft, The Netherlands.

^d Centre for Structural Biology, Institute of Fundamental Sciences, Massey University, Palmerston North, New Zealand.

Characterization of $\text{Na}_{12}[\text{Pd}_{0.4}\text{Na}_{0.6}\text{Pd}_{15}\text{P}_{10}\text{O}_5\text{H}_{6.6}]\cdot 36\text{H}_2\text{O}$ (Na-Pd₁₅).

1. General methods and materials. The reagents were used as purchased without further purification. Elemental analyses were performed by Mikroanalytisches Labor Pascher, Remagen, Germany. ³¹P NMR spectra were recorded on a 400 MHz JEOL ECX instrument at room temperature using 5-mm tube in H₂O / D₂O solution. The crystal water content was determined by thermogravimetric analysis (TGA) on a TA Instruments Q 600 device. Infrared spectra were recorded on KBr disks using a Nicolet-Avatar 370 spectrometer.

2. X-ray crystallography. Data for the structure of Na-Pd₁₅ were collected at 173 K on a Bruker Kappa X8 APEX CCD single-crystal diffractometer equipped with a sealed Mo tube and graphite monochromator ($\lambda = 0.71073 \text{ \AA}$). Crystals were mounted in Hampton cryoloops with light oil. The crystals were plate-like and most were obviously composite.

Semi-empirical absorption corrections were applied based on intensities of equivalent reflections with SADABS program.¹ The structure of Na-Pd₁₅ was solved by direct methods and refined by full-matrix least-squares against $|F|^2$ using the SHELXTL program package.² All atoms were refined anisotropically, except the oxygen atoms of the crystal waters. The site occupancy factors for these oxygen atoms were refined and then fixed at the obtained values. The hydrogen atoms of the crystal waters were not localized. The relative site occupancy factors (s.o.f.) for the disordered positions of Pd and Na in Na-Pd₁₅ were refined isotropically to values of 0.45 (~0.4) for Pd and 0.55 (~0.6) for Na. In the final anisotropic refinements, free variables were assigned to the Pd occupancy in two sites and the Na occupancy in one site and the sum of occupancies tightly restrained to a total occupancy of 1.0. Two of the Na of the water-cation structure are present in half occupancy along with coordinated water molecules. Refinements with full occupancy led to higher values for *R*₁ and *wR*₂ and the final stoichiometry of 12 Na in 13 sites is fully consistent with the microanalytical data. The very high value for *R*(int) on merging the data compared to *R*(sigma) (0.18 cf 0.08), numerous violations of systematic absences and the high *wR*₂ are consistent with the crystal having at least one "friend", especially as structure solution and refinement in lower symmetry space groups did not yield an improved model. As we were unable to discern any pattern in the list of reflections for which $F(\text{obs}) \gg F(\text{calc})$, we were not able to systematically remove composite reflections. Calculations of void volumes with PLATON (Spek, A.L. (2003), J.Appl.Cryst. 36, 7-13) revealed two equal void volumes totalling 876 Å³ (~8% of the unit cell volume) and containing ~300 electrons (~30 water molecules) in total. Calculations continued with SQUEEZEd data improved *R*₁ and especially

$wR2$. Nonetheless, the list of reflections showing poor agreement between $F(\text{obs})$ and $F(\text{calc})$ was populated only with reflections for which $F(\text{obs}) \gg F(\text{calc})$. Therefore, in final refinements, ~120 of these reflections were removed (<1% of total). This left the list of reflections showing poor agreement between $F(\text{obs})$ and $F(\text{calc})$ now containing some reflections for which $F(\text{obs})$ were less than $F(\text{calc})$. In view of the data infelicities, the suggested weighting scheme was partly ignored, and the second term in the weighting scheme was fixed at 115. Full justification for these crystallographic shenanigans is manifest in improved internal consistency of the numerous chemically near-equivalent bond parameters.

3. Electrochemistry of Na-Pd₁₅.

(a) Materials, apparatus, procedures. The solutions were deaerated thoroughly for at least 30 min with pure argon and kept under a positive pressure of this gas during the experiments. The source, mounting and polishing of the glassy carbon (GC, Le Carbone Lorraine, France) electrodes have been described.³ Controlled potential coulometry was carried out with a large surface area glassy carbon plate. The electrochemical set-up was an EG & G 273 A driven by a PC with the M270 software. Potentials are quoted against a saturated calomel electrode (SCE). The counter electrode was a platinum gauze of large surface area. All experiments were performed at room temperature.

Spectra were recorded with a Lambda 19 Perkin Elmer spectrophotometer. All solutions were 30 μM in POM and were placed in quartz cuvettes with an optical path of 1 cm.

The composition of the aqueous pH 7 medium was 0.4 M ($\text{NaH}_2\text{PO}_4 + \text{NaOH}$). Pure dioxygen (N48, Air Liquide, France) was bubbled through the solution for electrocatalytic studies and a blanket of this gas was maintained over the solution during experiments.

(b) Stability studies of Na-Pd₁₅.

Before studying the redox properties of **Na-Pd₁₅**, it was necessary to determine its stability domain over the pH scale being used. In fact, it is known that POMs may undergo chemical transformations or completely decompose depending on the pH of the solution in which they are dissolved.

For the stability tests, UV-Vis spectra of POM-containing solutions were recorded between 1200 nm and 200 nm as a function of time over a period of at least 10 h. The spectrum of **Na-Pd₁₅** was characterized by well-defined peaks located at 450 nm and 262 nm respectively. In the pH 7 (0.4 M ($\text{NaH}_2\text{PO}_4 + \text{NaOH}$)) the spectrum of **Na-Pd₁₅** was reproducible with respect to absorbances and peak wavelengths.

(c) Electrochemistry of Na-Pd₁₅. Figure S1A shows the very first cyclic voltammogram (CV) registered in a solution of **Na-Pd₁₅** between + 0.050 V and – 0.850 V. A crossover loop is observed in this CV because the current keeps growing upon changing the scan direction from negative to positive going potential and finally becomes much larger than the negative going branch. This observation indicates the formation and growth of a new phase following a nucleation event. It features the deposition of Pd⁰ on the electrode surface. From the second voltammetric run onward, the electroreduction of **Na-Pd₁₅** becomes easier. A composite voltammetric pattern began to develop between – 0.250 V and – 0.680 V (Fig. S1B). In particular, a well-defined cathodic peak (located at -0.658V) with an associated anodic peak appeared in this domain. On subsequent runs, the peak currents of this redox couple increased at every other scan. These scans ensured the formation of thicker and thicker Pd⁰ films in agreement with previous observations.⁴ Alternatively, film deposition can be realized by potentiostatic electrolysis. After deposition of a film on the glassy carbon surface, the electrode was taken out of the solution, copiously rinsed with Millipore water and used to run CV in the pure supporting electrolyte (pH 7). Figure S2 shows a representative example of the recorded CV which has essentially the same characteristics as those observed for Pd⁰ deposits on a glassy carbon electrode from Pd^{II} solutions.⁴ For the sake of clarity, the phenomena observed in the positive and negative potential domains will be described separately. As expected, the pattern observed between – 0.140 V and -0.730 V (Fig. S2A) exhibits the different states of hydrogen sorption-desorption processes.⁴ The sharp cathodic peak with a sharp and narrow anodic counterpart stands in contrast with the relatively larger asymmetry of the same process in the case of uncomplexed Pd^{II} ions.⁴ These characteristics might be assumed to establish faster electrochemical kinetic reactions on Pd⁰ deposited from **Pd₁₅**. In the domain starting from - 0.140 V to + 0.830 V in the positive potential direction and back to - 0.140 V, appears the two step oxidation of the deposited Pd surface followed by reduction of the oxide (Fig. S2B).

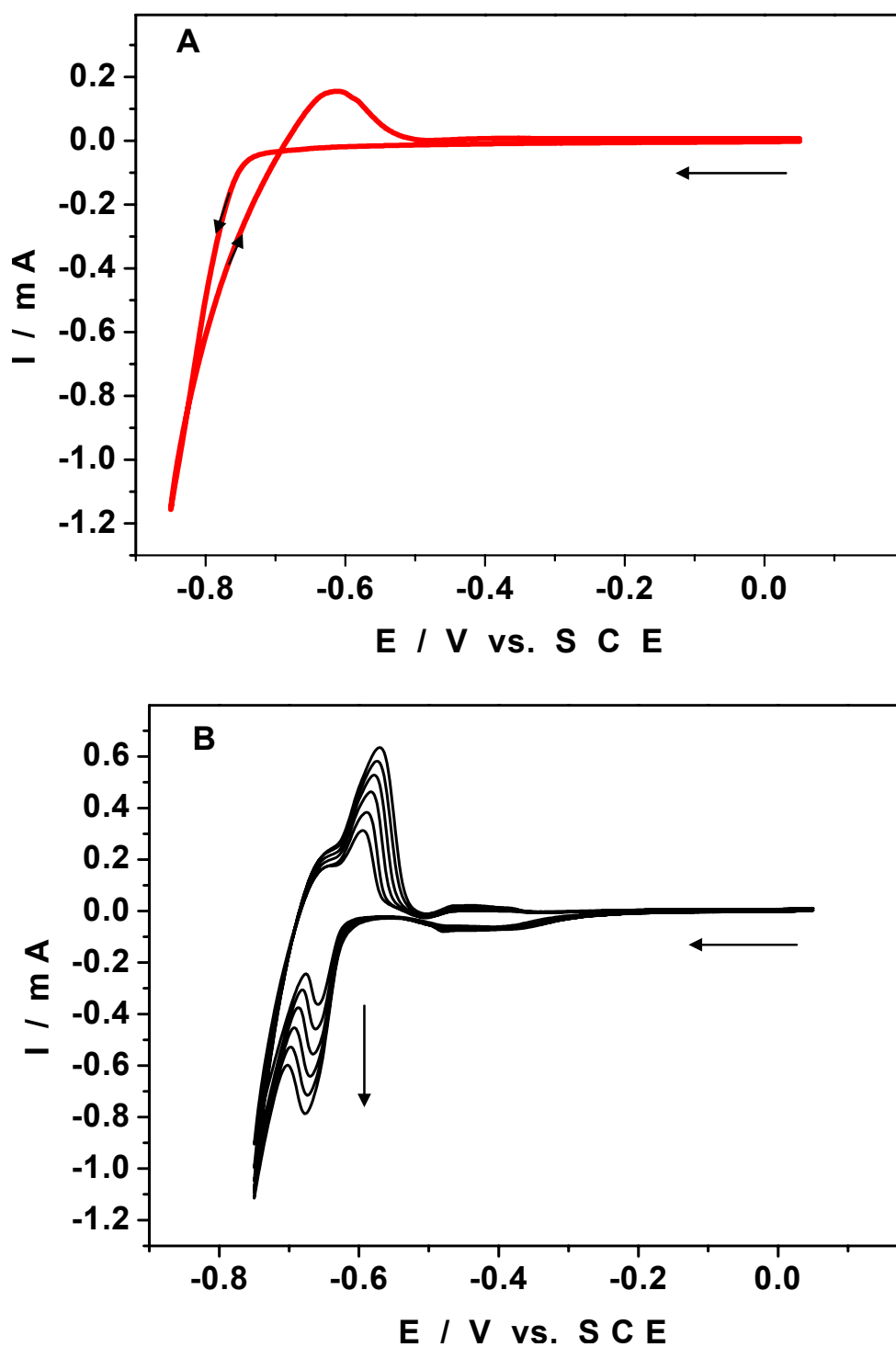


Figure S1. Cyclic voltammetry characterization of 4×10^{-5} M Na-Pd₁₅ solution in 0.4 M (NaH₂PO₄ + NaOH), pH = 7. The working electrode was a glassy carbon plate. The potentials are quoted against a saturated calomel electrode (SCE). The scan rate was 2 mVs^{-1} .

(A) First cycle showing the early stages of the deposition process.

(B) Evolution of cyclic voltammograms during a few runs (2nd through 8th cycle); the last cathodic peak current increases steadily for every consecutive run.

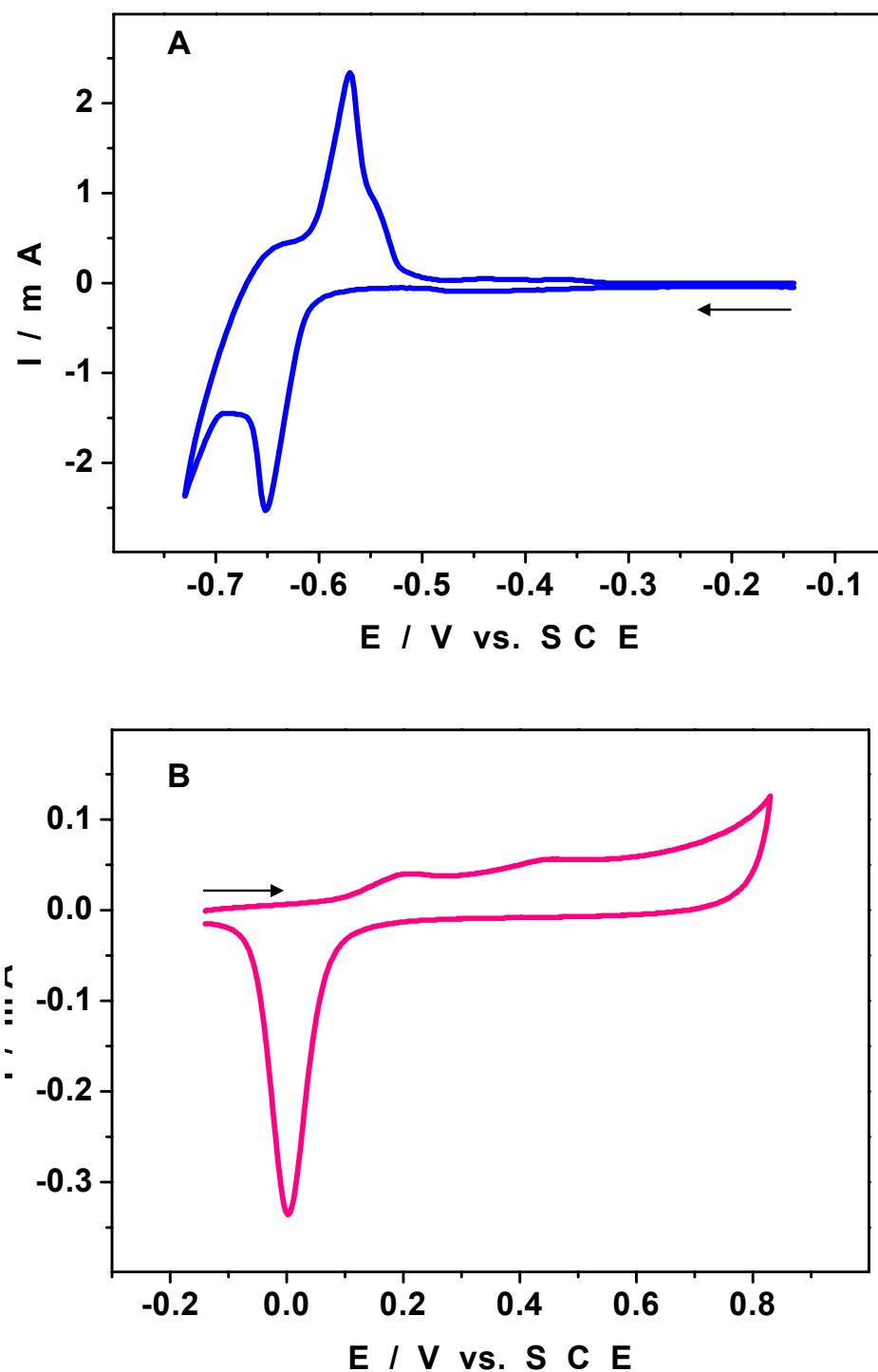


Figure S2. Cyclic voltammetry characterization of a thick film of **Na-Pd₁₅** in a pure supporting electrolyte (0.4 M (NaH₂PO₄ + NaOH) pH = 7). The working electrode was a glassy carbon plate. The potentials are quoted against a saturated calomel electrode (SCE). The scan rate was 2 mV s⁻¹.

(A) The electrode potential was scanned from -0.140 V to -0.730 and back.

(B) The electrode potential was scanned from -0.140 V to +0.730 V and back.

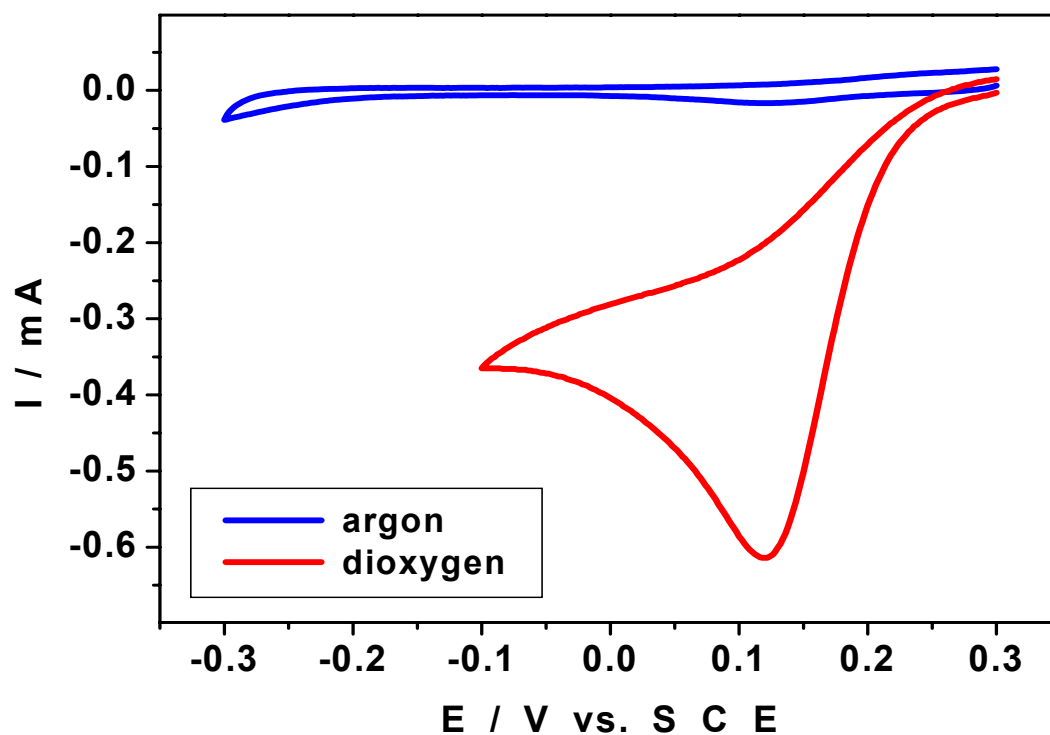


Figure S3. Cyclic voltammetry characterization, in (0.4 M (NaH₂PO₄ + NaOH) pH = 7 buffer, of the electrocatalytic reduction of dioxygen with a film of Pd⁰ deposited from a solution of Na-Pd₁₅ on a glassy carbon electrode. The potentials are quoted against a saturated calomel electrode (SCE). The scan rate was 2 mVs⁻¹. The voltammograms were obtained in a pure supporting electrolyte in the presence of argon or dioxygen, respectively.

4. ^{31}P NMR spectra of $[\text{Pd}_{0.4}\text{Na}_{0.6}\text{Pd}_{15}\text{P}_{10}\text{O}_{50}\text{H}_{6.6}]^{12-}$ (**Pd₁₅**).

^{31}P NMR spectra were recorded for **Na-Pd₁₅** redissolved in $\text{H}_2\text{O} / \text{D}_2\text{O}$ at room temperature, at 60 °C and then again at room temperature. All three obtained spectra are identical and show four signals (at 19.61, 19.55, 19.45 and 19.26 ppm) with approximate relative intensities 1 : 2 : 7 : 1 (Fig. S4).

The crystal structure of **Na-Pd₁₅** contains polyanions $[\text{Pd}_{15}\text{P}_{10}\text{O}_{50}\text{H}_x]^{(20-x)-}$, the central cavity of which is capped either by Na^+ (~60%) or by Pd^{II} (~40%). In the latter case the Pd^{II} ion is displaced from the central C_5 axis and coordinates only four oxygen atom of the pentagonal face of the inner $\{\text{O}_{10}\}$ polyhedron, which leads to a reduction of the D_{5h} symmetry of the polyoxopalladate to C_s (see Fig. 2 in the main text).

The successful repeated recrystallization of **Na-Pd₁₅** from aqueous media together with UV spectroscopy data suggest that the cyclic $\{\text{Pd}_{15}\text{P}_{10}\}$ polyoxopalladate core is stable in aqueous solution. As a result of the above described crystallographic disorder we propose the presence of the following species in solutions of **Na-Pd₁₅**:

- The “empty” polyoxopalladate shell $[\text{Pd}_{15}\text{P}_{10}\text{O}_{50}\text{H}_x]^{(20-x)-}$ (without any Na^+ or Pd^{II} caps): all 10 P atoms are chemically and magnetically equivalent and hence we expect a singlet. These polyanions can be formed easily by Na^+ -dissociation of $[\text{Na}\text{cPd}_{15}\text{P}_{10}\text{O}_{50}\text{H}_x]^{(19-x)-}$ or Pd^{II} -dissociation (perhaps also fluxionality) of $[\text{Pd}\text{cPd}_{15}\text{P}_{10}\text{O}_{50}\text{H}_x]^{(18-x)-}$. We attribute the strongest signal in our ^{31}P NMR spectrum at 19.45 ppm to the 10 equivalent phosphorous atoms in the “empty” polyanion $[\text{Pd}_{15}\text{P}_{10}\text{O}_{50}\text{H}_x]^{(20-x)-}$.

- The palladium-capped $[\text{Pd}\text{cPd}_{15}\text{P}_{10}\text{O}_{50}\text{H}_x]^{(18-x)-}$: This polyanion contains several chemically and magnetically inequivalent phosphorous atoms which lead to the appearance of several additional peaks in the ^{31}P NMR spectrum. The Pd^{II} ion coordinates only to one pole of the cyclic $\{\text{Pd}_{15}\text{P}_{10}\}$ assembly. We assume that the 5 phosphorous atoms from the “vacant” pole of $[\text{Pd}\text{cPd}_{15}\text{P}_{10}\text{O}_{50}\text{H}_x]^{(18-x)-}$ have the same chemical shift as the phosphorous atoms of $[\text{Pd}_{15}\text{P}_{10}\text{O}_{50}\text{H}_x]^{(20-x)-}$. The five P atoms from the opposite cap, which complexes the Pd^{II} ion, can be subdivided in three types with the ratio 1:2:2 (see Fig. S5). The first of them (shown in green colour in Fig. S5) could perhaps have the same chemical shift as P in the “empty” $\{\text{Pd}_{15}\text{P}_{10}\}$ polyanion shell. As a result we would expect the palladium-capped $[\text{Pd}\text{cPd}_{15}\text{P}_{10}\text{O}_{50}\text{H}_x]^{(18-x)-}$ to contribute 2 additional ^{31}P NMR signals compared to the “empty” polyoxopalladate shell $[\text{Pd}_{15}\text{P}_{10}\text{O}_{50}\text{H}_x]^{(20-x)-}$ described above.

- The sodium-capped $[\text{Na}\{\text{Pd}_{15}\text{P}_{10}\text{O}_{50}\text{H}_x\}]^{(19-x)-}$: This polyanion would result in two singlets of equal intensity in ^{31}P NMR, one of which (P of the non-coordinated cap) is expected to have the same chemical shift as the singlet of $[\text{Pd}_{15}\text{P}_{10}\text{O}_{50}\text{H}_x]^{(20-x)-}$. Therefore, the sodium-capped $[\text{Na}\{\text{Pd}_{15}\text{P}_{10}\text{O}_{50}\text{H}_x\}]^{(19-x)-}$ would contribute the fourth and last signal to the spectrum we see in Fig. S4.

Unfortunately, it is impossible to assign the three low-intensity signals to specific P atoms, but the observed ^{31}P spectrum supports the solution stability of the cyclic $\{\text{Pd}_{15}\text{P}_{10}\}$ polyoxopalladate core and its coordinated derivatives in aqueous solution.

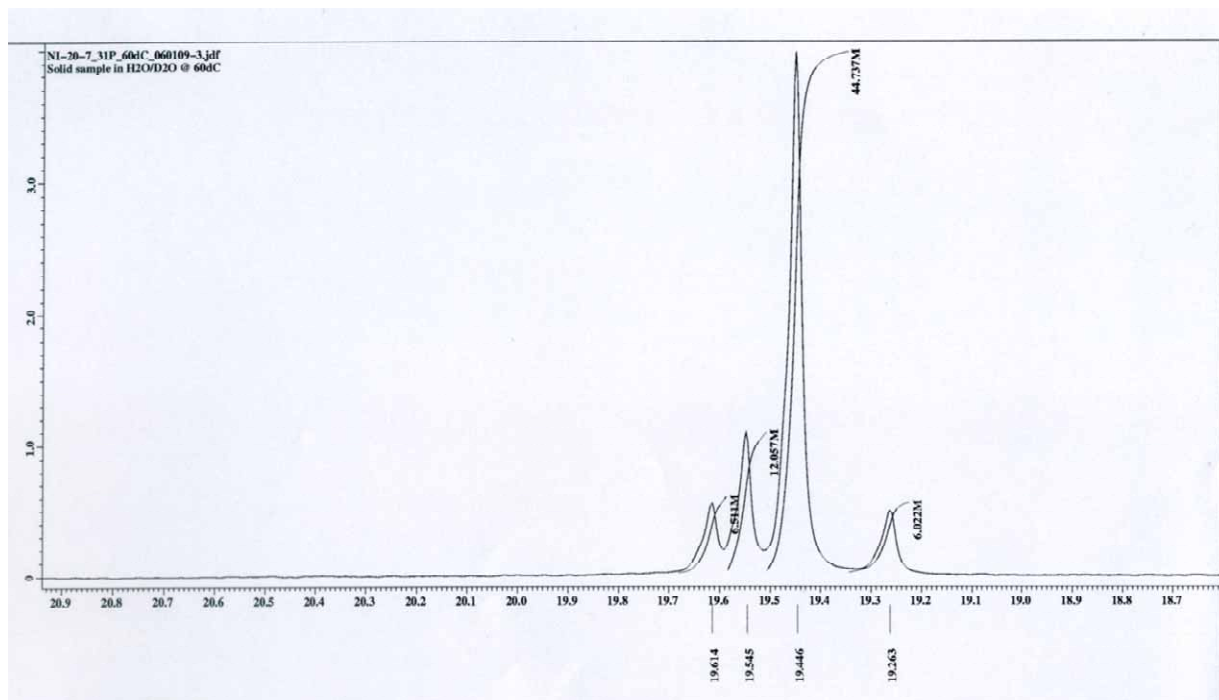


Figure S4. ^{31}P NMR spectra of an aqueous solution of Na-Pd_{15} .

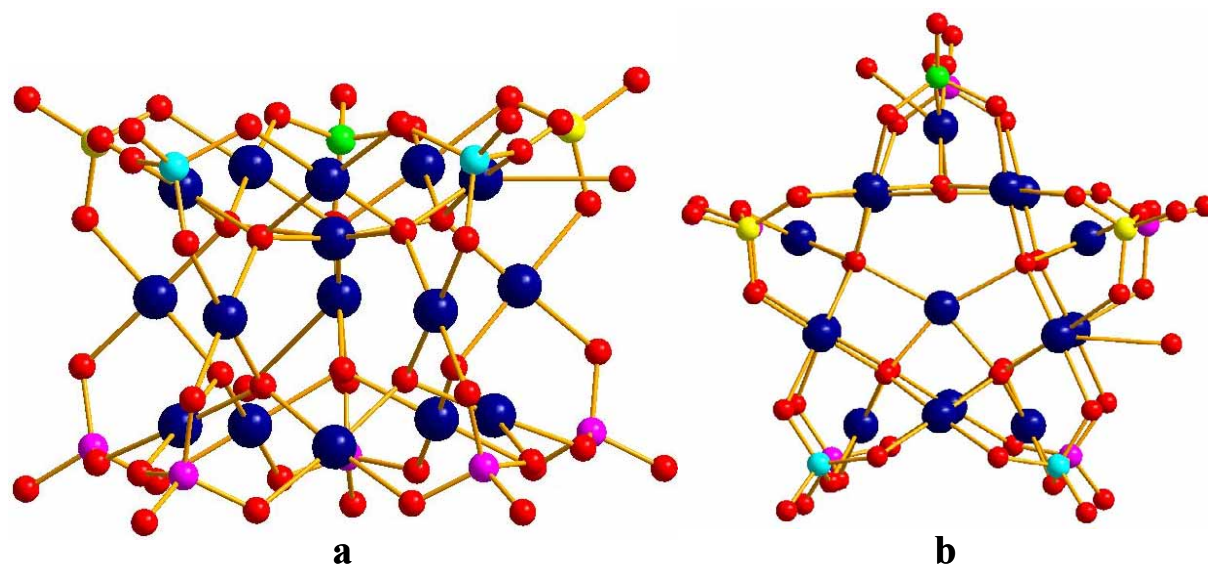


Figure S5. Ball-and-stick representation of $[\text{Pd}_{0.4}\text{Pd}_{15}\text{P}_{10}\text{O}_{50}\text{H}_x]^{(18-x)-}$ highlighting the chemically and magnetically inequivalent phosphorous heteroatoms by different colors. Colour code: Pd blue, O red, P pink / turquoise / yellow / green.

5. Thermogravimetric analysis for $\text{Na}_{12}[\text{Pd}_{0.4}\text{Na}_{0.6}\text{Pd}_{15}\text{P}_{10}\text{O}_{50}\text{H}_{6.6}]\cdot 36\text{H}_2\text{O}$ (Na-Pd₁₅**) from room temperature to 900 °C under N_2 atmosphere.**

The TGA curves of **Na-Pd₁₅** exhibit two weight loss steps (Fig. S6). The first step begins at 25 °C and is complete at 175 °C, which corresponds to the loss of all 36 water molecules per formula unit $\text{Na}_{12}[\text{Pd}_{0.4}\text{Na}_{0.6}\text{Pd}_{15}\text{P}_{10}\text{O}_{50}\text{H}_{6.6}]\cdot 36\text{H}_2\text{O}$ (**Na-Pd₁₅**). The weight loss of 17.4% is in excellent agreement with the calculated value of 17.6%. The smooth weight loss in the temperature range of 175 – 262 °C corresponds to the loss of 3.3 water molecules per formula unit **Na-Pd₁₅**, which must originate from $[\text{Pd}_{0.4}\text{Na}_{0.6}\text{Pd}_{15}\text{P}_{10}\text{O}_{50}\text{H}_{6.6}]^{12-}$ (**Pd₁₅**). This implies that the polyanion is being decomposed. The total observed weight loss at 900 °C is 26.4%.

6. The FR-IR spectrum of Na-Pd₁₅ (Fig. S7) shows strong bands at 616 and 548 cm^{-1} corresponding to the $[\text{PdO}_n]$ groups. The strong bands at 1094, 1081 and 953 cm^{-1} are attributed to the phosphate heterogroups, and the broad band at 1652 cm^{-1} is due to crystal waters.⁵

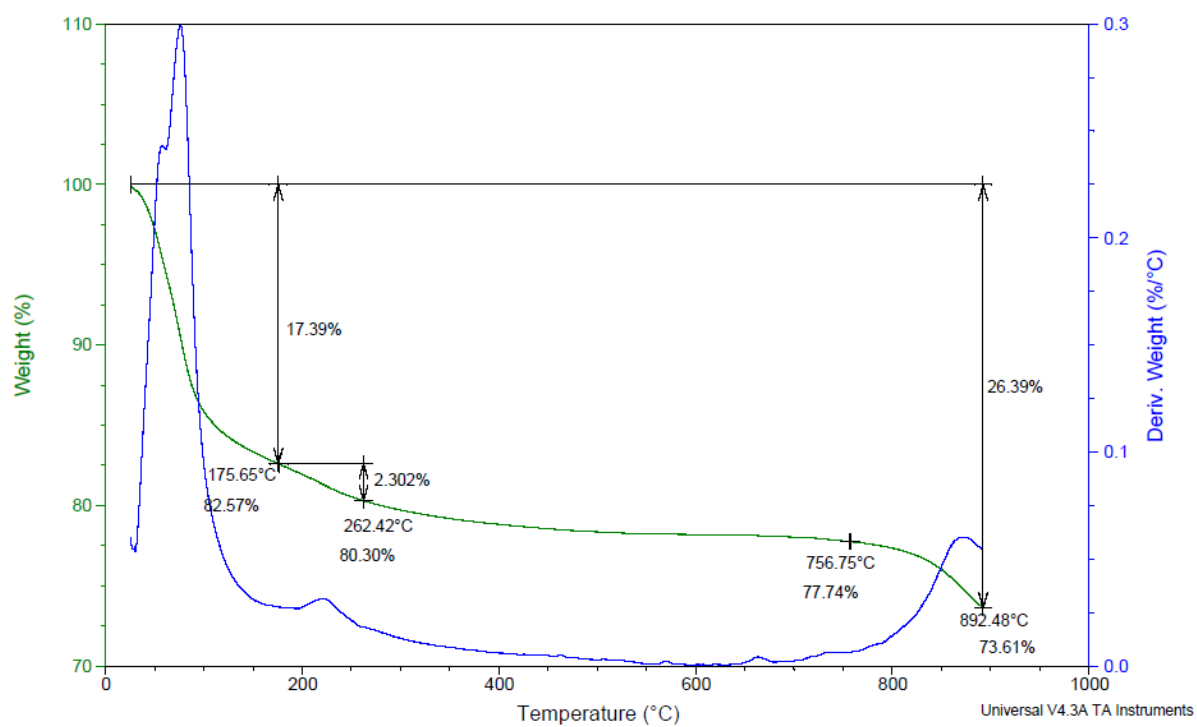


Figure S6. Thermogravimetric analysis for Na-Pd_{15} from room temperature to 900 °C under N_2 atmosphere.

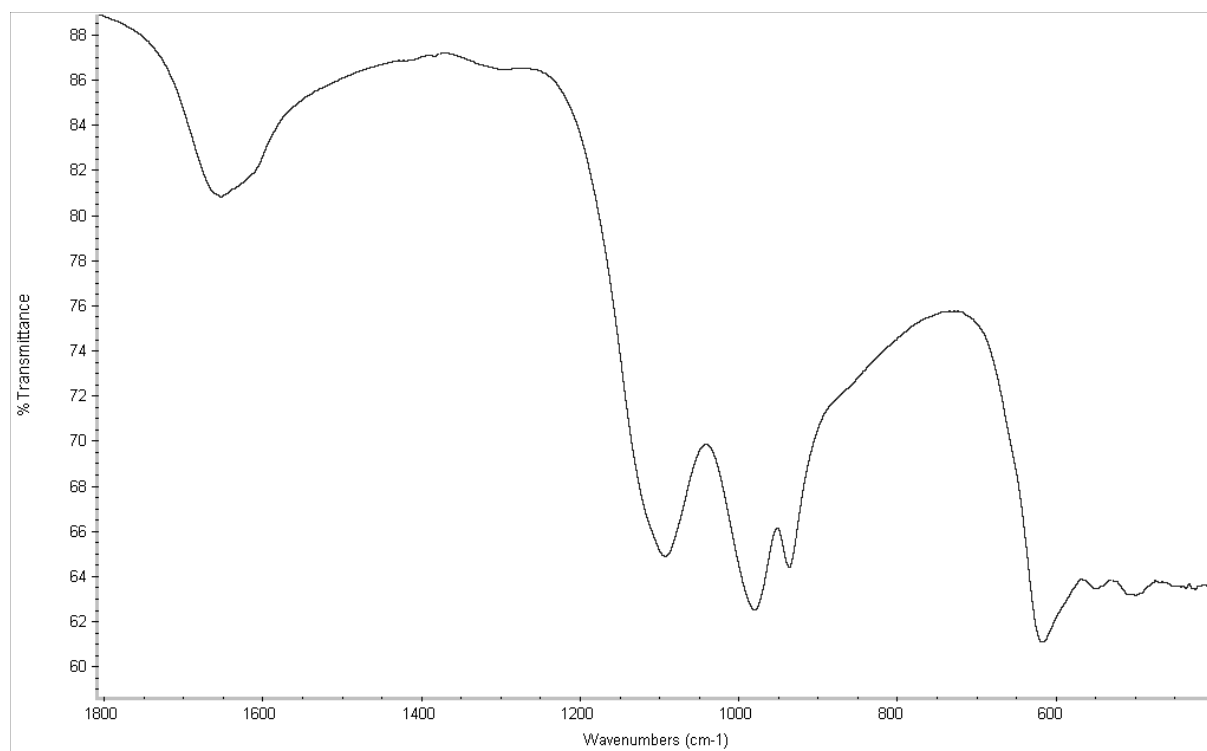


Figure S7. FT-IR spectrum of Na-Pd₁₅.

References

1. G.M. Sheldrick, SADABS, *Program for empirical X-ray absorption correction*, Bruker-Nonius, 1990.
2. G.M. Sheldrick, *Acta Crystallogr.* 2007, **A64**, 112.
3. B. Keita and L. Nadjo, *J. Electroanal. Chem.* 1988, **243**, 87.
4. (a) L.-H. Bi, M. Reicke, U. Kortz, B. Keita, L. Nadjo and R.J. Clark, *Inorg. Chem.* 2004, **43**, 3915 (and references therein); (b) L.-H. Bi, U. Kortz, B. Keita, L. Nadjo and H. Borrmann, *Inorg. Chem.* 2004, **43**, 8367; (c) L.-H. Bi, U. Kortz, B. Keita, L. Nadjo and L. Daniels, *Eur. J. Inorg. Chem.* 2005, 3034; (d) T.M. Anderson, R. Cao, E. Slonkina, B. Hedman, K.O. Hodgson, K.I. Hardcastle, W.A. Neiwert, S. Wu, M.L. Kirk, S. Knottenbelt, E.C. Depperman, B. Keita, L. Nadjo, D.G. Musaev, K. Morokuma and C.L. Hill, *J. Am. Chem. Soc.* 2005, **127**, 11948; (e) T.M. Anderson, R. Cao, E. Slonkina, B. Hedman, K.O. Hodgson, K.I. Hardcastle, W.A. Neiwert, S. Wu, M.L. Kirk, S. Knottenbelt, E.C. Depperman, B. Keita, L. Nadjo, D.G. Musaev, K. Morokuma and C.L. Hill, *J. Am. Chem. Soc.* 2008, **130**, 2877 (addition/correction); (f) E.V. Chubarova, M.H. Dickman, B. Keita, L. Nadjo, F. Misereque, M. Misfud, I.W.C.E. Arends and U. Kortz, *Angew Chem. Int. Ed.*, 2008, **47**, 9542.
5. K. Nakamoto, *Infrared and Raman Spectra of Inorganic and Coordination Compounds- Part A: Theory and Applications in Inorganic Chemistry*, 5th ed.; Wiley and Sons, New York, 1997.